

Original Article

MicroRNA-876-3p functions as a tumor suppressor gene and correlates with cell metastasis in pancreatic adenocarcinoma via targeting JAG2

Fu Yang^{1*}, Wan Jun Zhao^{2*}, Cong Li Jia³, Xiao Kai Li¹, Qiang Wang¹, Zi Li Chen⁴, De Quan Jiang⁵

¹Department of Hepatobiliary Surgery, First Affiliated Hospital of Kunming Medical University, Kunming, Yunnan, China; ²The Department of Thyroid Surgery, West China Hospital, Sichuan University, Chengdu, Sichuan, China; ³Huize Ren An Hospital, Department of General Surgery, Qujing, Yunnan, China; ⁴Department of Hepatobiliary Surgery, Affiliated Hospital of Guizhou Medical University, Guiyang, Guizhou, China; ⁵The Second Department of General Surgery of Jiangjin Center Hospital, Chongqing, China. *Equal contributors.

Received February 9, 2018; Accepted February 20, 2018; Epub April 1, 2018; Published April 15, 2018

Abstract: Dysregulation of microRNA (miRNA) expression in multiple cancers and their vital roles in malignant cancer progression are well investigated. The purpose of this study was to explore the biological roles of miR-876-3p in pancreatic cancer. We used genome-wide gene expression analysis in clinical pancreatic adenocarcinoma samples to identify miR-876-3p down-regulated in pancreatic cancer. We then collected 22 pairs of pancreatic cancer and the corresponding non-cancerous tissues to determine miR-876-3p level, and confirmed that miR-876-3p was significantly down-regulated in pancreatic cancer. Furthermore, functional analysis suggested that overexpression of miR-876-3p suppressed cell growth and aggressively increased cells apoptosis in BXPc-3 and PANC-1 cells, whereas down-regulation led to the opposite results. We identified Jagged2 (JAG2) as a direct target of miR-876-3p, and an inverse correlation between miR-876-3p and JAG2 was observed in pancreatic adenocarcinoma. Moreover, miR-876-3p and a JAG2 siRNA were co-transfected into both PANC-1 and BXPc-3 cells to explore the mechanism of miR-876-3p and JAG2 on pancreatic adenocarcinoma tumorigenesis. Down-regulation of JAG2 inhibited the overexpression effects of miR-876-3p, and up-regulation of JAG2 reversed the effects of overexpressed miR-876-3p. Cumulatively, these results revealed a significant role of the miR-876-3p/JAG2 axis in suppressing pancreatic adenocarcinoma cell growth and aggressiveness.

Keywords: miR-876-3p, JAG2, pancreatic adenocarcinoma, aggressiveness

Introduction

Pancreatic adenocarcinoma is a serious neoplasm, with a 5-year survival rate lower than 5% [1, 2]. Despite improvements in early diagnosis, surgical techniques, and chemotherapy, the local infiltration and distant metastasis primarily accounts for the poor prognosis of patients with pancreatic cancer [3]. Unfortunately, little is known concerning the reasons for the aggressiveness of and dismal prognosis for pancreatic cancer. Therefore, it is crucial to investigate the mechanisms that regulate pancreatic cancer metastasis in order to improve pancreatic cancer treatment [4]. During the metastatic process, the primary cancer cells undergo the following steps sequentially: invasion, intravasation, survival in circulation, extravasation

into distant tissues, and colonization at secondary sites [5, 6]. To prevent cancer metastasis, it is essential to identify the mechanisms triggering the pancreatic cancer metastatic process.

MicroRNA (miRNA) is a small non-coding RNA that regulates gene expression by inhibiting mRNA translation [7]. miRNAs are usually down-regulated in various kinds of human cancers, suggesting that they act as tumor suppressors. A substantive amount of research demonstrates that dysregulated miRNAs are associated with cancer cell proliferation, apoptosis, invasion, and chemo-sensitivity [8]. The overexpression of JAG2 was first identified in malignant plasma cells from patients with multiple myeloma [9]. Up-regulation of JAG2 was also identified in various cancers, including

bladder, breast, lung, and ovarian cancers, and is closely related with the progression of these tumors [10]. A previous study reports that the expression of JAG2 is increased in human colorectal cancer when compared to that in the corresponding normal tissues, which suggests that JAG2 plays crucial roles in colorectal cancer cell growth and progression [11]. Similar pro-metastatic functions were demonstrated for JAG2 in other types of cancer. In breast cancer, JAG2 promotes metastasis, and its expression is significantly associated with overall and metastasis-free survival of breast cancer patients [12]. Likewise, JAG2 is also found to be capable of accelerating the metastasis of lung adenocarcinoma cells in mice [13]. Altogether, these findings support the hypothesis that JAG2 functions to promote metastasis in multiple cancer types. However, the precise mechanisms by which signaling responses contribute to JAG2-mediated pancreatic carcinogenesis and metastasis remain to be elucidated.

In the present study, we identified miR-876-3p to be down-regulated in pancreatic cancer and also determined that miR-876-3p acted as an important suppressor of pancreatic cancer. The bioinformatic analysis and luciferase assay demonstrated that JAG2 was the direct target of miR-876-3p. Overexpression of miR-33a led to a marked down-regulation of JAG2 expression, which in turn inhibited pancreatic cancer cell growth and suppressed the metastasis of pancreatic cancer cells, both *in vitro* and *in vivo*. However, down-regulation of miR-33a resulted in the opposite results. To conclude, our results provide novel insights into the mechanism of the miR-876-3p/JAG2 axis in pancreatic cancer and suggest therapeutic strategies for this malignancy.

Materials and methods

Pancreatic cancer cell lines and tissues

Samples of pancreatic carcinoma and normal tissues were collected from the first affiliated hospital of Kunming medical university. The pancreatic carcinoma tissues and normal tissues were rapidly frozen in liquid nitrogen and stored at -80°C . Tissue sections ($4\text{-}\mu\text{m}$ thick) were non-specifically blocked with goat serum, followed by overnight incubation with anti-JAG2 (1:100; Beyotime Biotechnology, Nanjing, Ch-

ina) and then incubated with Cy3-labelled or FITC-labelled secondary antibodies (Beyotime Biotechnology) at room temperature for 1.5 h. Finally, the sections were counterstained with DAPI for 10 min, and observed under a fluorescence microscope. SW1990, AsPC-1, BXPC-3, PANC-1, and the pancreatic ductal cell line HPDE6-C7 used in the study were purchased from Cobioer (Nanjing, China). The cells were cultured in RPMI-1640 or DMEM with 10% FBS (Gibco, USA) and supplemented with penicillin/streptomycin (Sigma, USA) at 37°C in an atmosphere containing 5% CO_2 and 95% air.

Cell transfection

Both PANC-1 and BXPC-3 cells were transfected with miR-876-3p mimic (Ambion, Austin, TX, USA) or anti-miR-876-3p (Ambion) via the reverse transfection method using the siPORT NeoFX transfection reagent (Ambion). The siRNA targeting human JAG2 (si-JAG2) and the corresponding negative control were purchased from GenePharma (Shanghai, China). JAG2 overexpressing plasmids were constructed using pCDNA3.1(+) basic vectors by GenePharma. Plasmids were transfected into PANC-1 and BXPC-3 cells using Lipofectamine 2000 (Invitrogen, USA).

Cell proliferation and apoptosis assay

The growth of indicated the cells was determined using 3-(4,5-dimethyl-2-thiazolyl)-2,5-diphenyl-2-H-tetrazolium bromide (MTT) assay. BXPC-3 and PANC-1 cells (2×10^3 cells in $100\ \mu\text{L}$) were seeded into 96-well plates. Four hours after transfection, the medium was renewed and then cultured for 24 h, 48 h, 72 h, and 96 h. MTT solution ($100\ \mu\text{L}$) was added to each well and incubated for 4 h at 37°C . An automatic microplate reader (BioTeke, China) detected the absorbance at 450 nm. Apoptotic rates of PANC-1 and BXPC-3 were analyzed using an Annexin V-Alexa Fluor/PI apoptosis detection kit (Beyotime Biotechnology) according to the manufacturer's specifications [14].

Wound healing and invasion assay

Cells were seeded into 6-well plates, and a scratch was made using a sterile pipette tip. The medium was removed and replaced with serum-free medium. The ability of the cells to close the wound was determined by comparing

miR-876-3p inhibits pancreatic adenocarcinoma progression

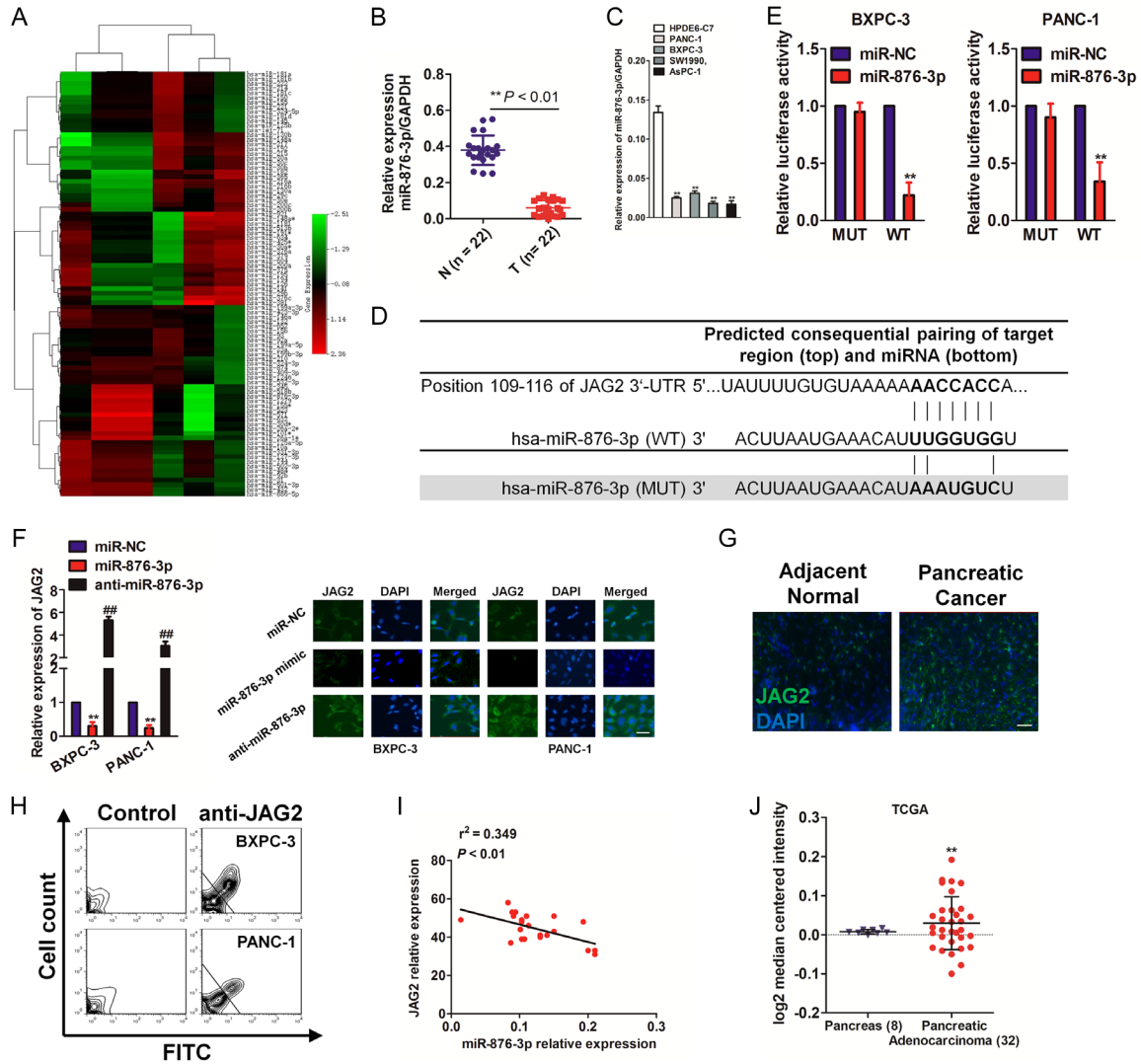


Figure 1. MiR-876-3p is down-regulated in pancreatic cancer samples and cell lines. **A.** Microarray analysis of miRNA expression in pancreatic cancer tissues from normal pancreatic tissues. **B.** The level of miR-876-3p in 22 adjacent normal control tissues (N) and 22 pancreatic cancer tissues (T) was determined by qRT-PCR. **C.** qRT-PCR analyzed the levels of miR-876-3p in pancreatic cancer cell lines. GAPDH was used as loading control. **D.** Schematic diagram of miR-876-3p binding sites in the JAG2 3'-UTR. Sequences were compared between the mature miR-876-3p and wild-type (WT) or mutant (MUT) putative target sites in the 3'-UTR of JAG2. **E.** BXPC-3 and PANC-1 cells were co-transfected with the wild-type (WT) or mutant (MUT) JAG2 3'-UTR with miR-876-3p and the luciferase activity was examined. Firefly luciferase activity was measured and standardized by Renilla luciferase activity. **F.** BXPC-3 and PANC-1 cells were transfected with miR-876-3p and anti-miR-876-3p. JAG2 expression as determined by qRT-PCR (left panel) and immunofluorescence assays (right panel). **G.** Immunofluorescence staining of JAG2 in normal human pancreatic cancer tissue and corresponding normal tissues. Scale bars represent 50 μ m. **H.** Representative FACS dot plots of BXPC-3 and PANC-1 cells stained with an anti-JAG2 antibody (right) or with an isotype matched antibody (as a background control, left). **I.** The expression correlation analysis of miR-876-3p and JAG2 in tumor samples was conducted by qRT-PCR assay. **J.** Box plots derived from gene expression data in Oncomine comparing expression of JAG2 gene in normal (left plot) and pancreatic cancer tissue (right plot).

the 0-h and 24-h phase contrast micrographs. BXPC-3 or PANC-1 cells (2×10^4) were added to the top of a 24-well Millipore transwell chamber (Millipore, USA), and 600 μ L of medium con-

taining 10% FBS was added to the lower chamber. After 24 h, the cells in the lower chamber were stained with crystal violet (Sigma, USA) [15, 16].

Luciferase reporter assay

The wild-type (WT) or mutant (MUT) 3'-UTR of JAG2 containing the miR-876-3p binding site was cloned into the dual-luciferase reporter, psiCHECK™-2 vector (Promega, USA). In the dual-luciferase reporter assay, BxPC- or PANC-1 cells were transfected with miR-876-3p or negative control (NC) for 24 h and the cells were then transfected with the WT/MUT-JAG2-3'-UTR reporter plasmid using Lipofectamine 2000 (Invitrogen). After 48 h, the luciferase activities were conducted using the dual-luciferase reporter assay kit (Promega, USA) [17].

Quantitative real-time PCR (qRT-PCR) assay

Pancreatic cancer tissues and cells were subjected to total RNA extraction using TRIzol reagent (Takara, Japan). Complementary DNA (cDNA) was synthesized using the ABI 9700 PCR amplifier system (Applied Biosystems, USA). The primer sequences are as follows: JAG2, forward primer: 5'-TGGGCGGCAACTCCTTCTA-3', reverse primer: 5'-GCCTCCACGATGAGGGTAAA-3'; Ki67, forward primer: 5'-TTCGC-AAGCGCATAACCCA-3', reverse primer: 5'-AACC-GTGTACAGTGCCAAA-3'; GAPDH, forward primer: 5'-TGGATTTGGACGCATTGGTC-3', reverse primer: 5'-TTTGAAGTCTGGTACGTGTTGATA-3'. The miRNA and mRNA expression levels were normalized to GAPDH.

Immunofluorescence

Cells were fixed in 4% formaldehyde and permeabilized with 0.5% Triton X-100 for 10 min. Cells were then incubated overnight with anti-JAG2 antibody at 4°C, followed by incubation with Cy3-labelled or FITC-labelled secondary antibodies (Beyotime Biotechnology) at room temperature for 1.5 h. Finally, cells were counterstained with DAPI for 10 min, and observed under a fluorescence microscope.

In vivo animal experiments

BALB/c nude mice were subcutaneously inoculated with tumor cells (1×10^6 per mouse). Nude mice were sacrificed 25 days later and the tumors were removed. Tumor growth was determined by measuring the tumor volume ($V = 0.5 \times \text{tumor length} \times \text{tumor width}^2$) every 3 days using calipers. Tumor tissue sections were deparaffinized, rehydrated, and rinsed before

antigen retrieval and endogenous peroxidase blocking. Following blocking with goat serum, the sections were incubated with anti-Ki67 (1:100; Beyotime Biotechnology) primary antibody at 4°C. Standard DAB method (Beyotime Biotechnology) was employed to detect staining. Tail-injected animals were sacrificed 4 weeks after the injection, and their lungs were removed. Lung tissues were fixed in 10% buffered formalin, immersed in an ascending series of alcohol washes, and paraffin embedded. The tissues were then sectioned (4- μm thick) and stained with hematoxylin and eosin (H&E). All procedures involving mice were conducted in accordance with the Animal Care guidelines of the first affiliated hospital of Kunming medical university.

Statistical analyses

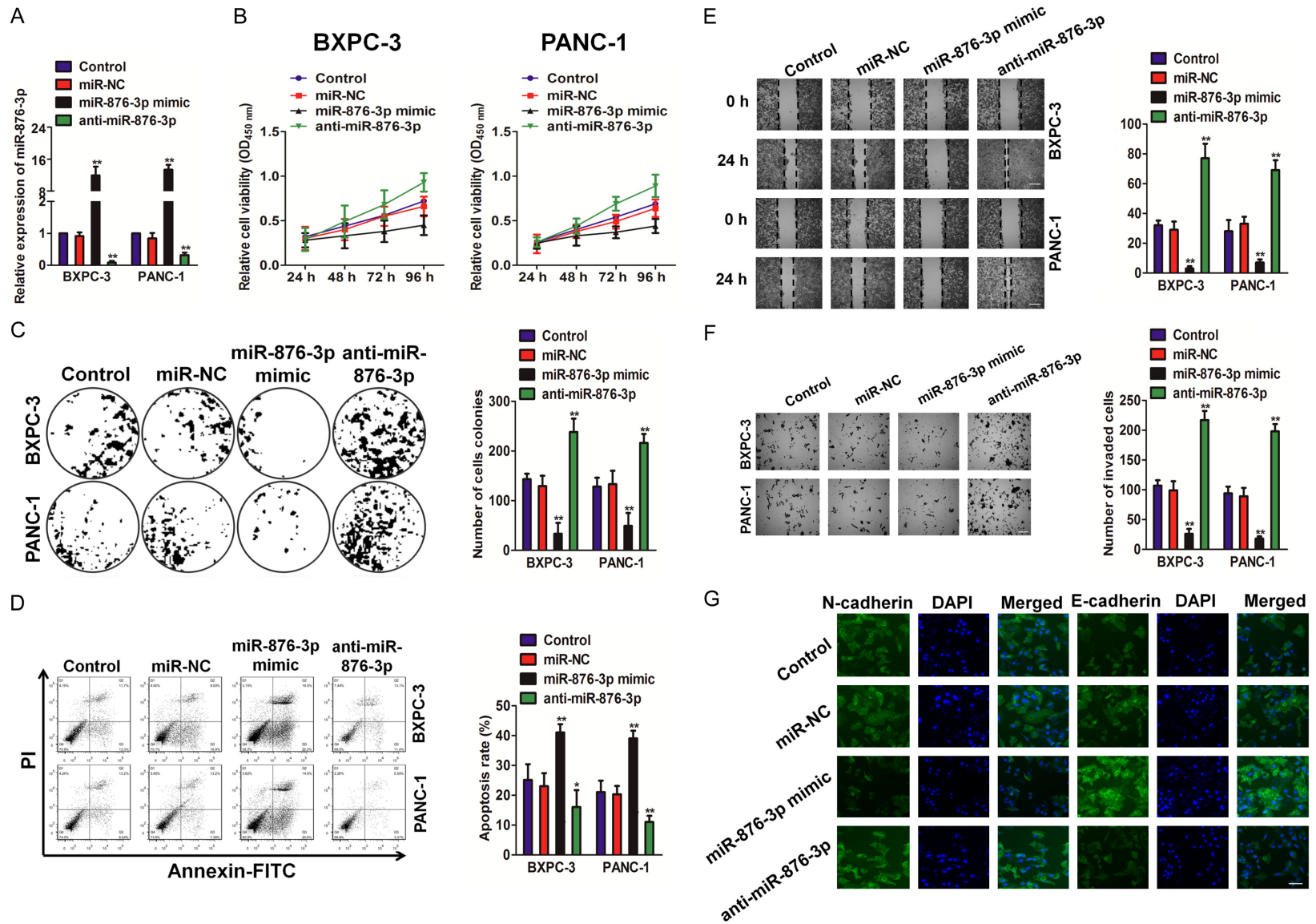
SPSS software was used to analyze the data with independent sample *t*-tests. All values were represented as mean \pm SD. $P < 0.05$ was considered to be statistically significant.

Results

MiR-876-3p expression is down-regulated in human pancreatic adenocarcinoma

To identify the potential miRNAs that were aberrantly expressed in pancreatic cancer, we compared the expression patterns of miRNAs in healthy individuals and pancreatic cancer patients using the GEO dataset, GSE24279. The heat map generated using differential genes showed that miR-876-3p was remarkably down-regulated in pancreatic cancer tissues (**Figure 1A** and **Supplementary Table 1**). Therefore, we first examined the differences in miR-876-3p expression between pancreatic adenocarcinoma and normal pancreas. To explore the potential biological role of the altered miR-876-3p expression in pancreatic cancer progression, we evaluated miR-876-3p expression in 22 pancreatic adenocarcinoma tissues and 22 normal pancreatic tissues using qRT-PCR. As shown in **Figure 1B**, miR-876-3p expression levels significantly decreased in the pancreatic cancer tissues when compared to normal tissues. Consistently, miR-876-3p expression also remarkably decreased in various pancreatic cancer cell lines (**Figure 1C**). We then used bioinformatics prediction softwares (miRanda, mirSVR and TargetScan) to determine the tar-

miR-876-3p inhibits pancreatic adenocarcinoma progression



miR-876-3p inhibits pancreatic adenocarcinoma progression

Figure 2. Effect of miR-876-3p in growth, migration and invasion in BXPC-3 and PANC-1 cells. A. Cells were transfected with miR-876-3p mimic or anti-miR-876-3p. The expression levels of miR-876-3p were detected by qRT-PCR. B. Cell proliferation rates were determined by the MTT assay. C. Colony formation assays of BXPC-3 and PANC-1 cells. Representative images for each treatment were shown. D. Both BXPC-3 and PANC-1 cells were transfected with miR-876-3p mimic or anti-miR-876-3p and the rate of apoptosis was analyzed by flow cytometry using Annexin V-FITC/PI kit. * $P < 0.01$, ** $P < 0.01$ as compared to control cells. E. miR-876-3p mimic or anti-miR-876-3p was transfected into BXPC-3 and PANC-1 cells. The ability of migration in pancreatic cancer cells was determined by wound closure assay. Scale bar: 200 μm . F. The invasion of indicated BXPC-3 and PANC-1 cells was determined by Transwell assay. ** $P < 0.01$ as compared to control cells. Scale bar: 200 μm . G. Immunofluorescence detection of E-cadherin and N-cadherin in cells transfected with miR-876-3p mimic or anti-miR-876-3p.

gets of miR-876-3p. We found that the Jagged-2 (JAG2) 3'-UTR had a sequence that bound to miR-876-3p at position 109-116 (**Figure 1D**). To verify that miR-876-3p targeted JAG2, the luciferase assay was conducted. The results showed that miR-876-3p significantly inhibited the luciferase activity of the 3'-UTR of JAG2 in pancreatic adenocarcinoma cells (**Figure 1E**). We also measured the level of miR-876-3p in cells transfected with the miR-876-3p mimic or anti-miR-876-3p via qRT-PCR. The expression of miR-876-3p inhibited the production of JAG2 mRNAs and proteins, whereas inhibition of miR-876-3p promoted the expression of JAG2 (**Figure 1F**). Next, we examined JAG2 protein levels via immunofluorescence staining in human pancreatic cancer tissues and corresponding normal pancreatic tissues, and revealed that JAG2 was overexpressed in pancreatic cancer (**Figure 1G**). FACS analysis after staining with anti-JAG2 antibody revealed the existence of distinct cell subpopulations expressing the gene (**Figure 1H**), compatible with the existence of a fraction of the cells expressing JAG2 at steady state. Finally, qRT-PCR analysis showed that miR-876-3p down-regulation was greatly correlated with the overexpression of JAG2 in pancreatic cancer tissues (**Figure 1I**). Oncomine analysis of neoplastic vs. normal tissue showed that JAG2 was significantly over-expressed in pancreatic adenocarcinoma in TCGA dataset (**Figure 1J**). These results suggested that miR-876-3p, which negatively regulated the expression of JAG2, was down-regulated in pancreatic cancer.

miR-876-3p plays a negative role in pancreatic cancer cell proliferation, mobility, and invasion

To investigate the role of miR-876-3p, pancreatic cancer cells were transfected with the miR-876-3p mimic or anti-miR-876-3p. As shown in **Figure 2A**, the transfected miR-876-3p mimic increased the levels of miR-876-3p, whereas anti-miR-876-3p suppressed the expression of

miR-876-3p in BXPC-3 and PANC-1 cells. After transfection with the miR-876-3p mimic or anti-miR-876-3p, cells were seeded into 96-well plates. After 24-h, 48-h, 72-h, and 96-h incubations, the MTT assay was performed to determine cell proliferation. We found that overexpression of miR-876-3p reduced both BXPC-3 and PANC-1 cell proliferation, whereas inhibition of miR-876-3p promoted BXPC-3 and PANC-1 cell proliferation when compared to control cells (**Figure 2B**). These results were consistent with the results obtained via the colony formation assay (**Figure 2C**), suggesting that miR-876-3p was involved in inhibiting pancreatic cancer cell growth in vitro. Next, we evaluated the effect of miR-876-3p on PANC-1 and BXPC-3 cell apoptosis. As shown in **Figure 2D**, apoptosis of BXPC-3 and PANC-1 cells increased after the miR-876-3p mimic transfection, whereas apoptosis decreased after the cells were transfected with anti-miR-876-3p. Wound healing and Transwell assays were performed to investigate the effects of miR-876-3p on pancreatic cancer cell migration and invasion in vitro. Overexpression of miR-876-3p inhibited cell migration and invasion, whereas anti-miR-876-3p transfection accelerated the mobility of pancreatic cancer cells in vitro (**Figure 2E, 2F**). Furthermore, immunofluorescence for the cell lines showed that over-expression of miR-876-3p inhibited the expression of N-cadherin and increased the level of epithelial marker (E-cadherin) whereas down-regulation of miR-876-3p caused the opposite results (**Figure 2G**).

Down-regulation of JAG2 and miR-876-3p over-expression exhibit similar effects

To investigate the biological functions of JAG2 in pancreatic cancer cells, endogenous JAG2 was knocked-down in BXPC-3 and PANC-1 cells with a specific siRNA against JAG2 (siJAG2). We found that JAG2 was significantly inhibited in BXPC-3 and PANC-1 cells by siJAG2 (**Figure 3A**).

miR-876-3p inhibits pancreatic adenocarcinoma progression

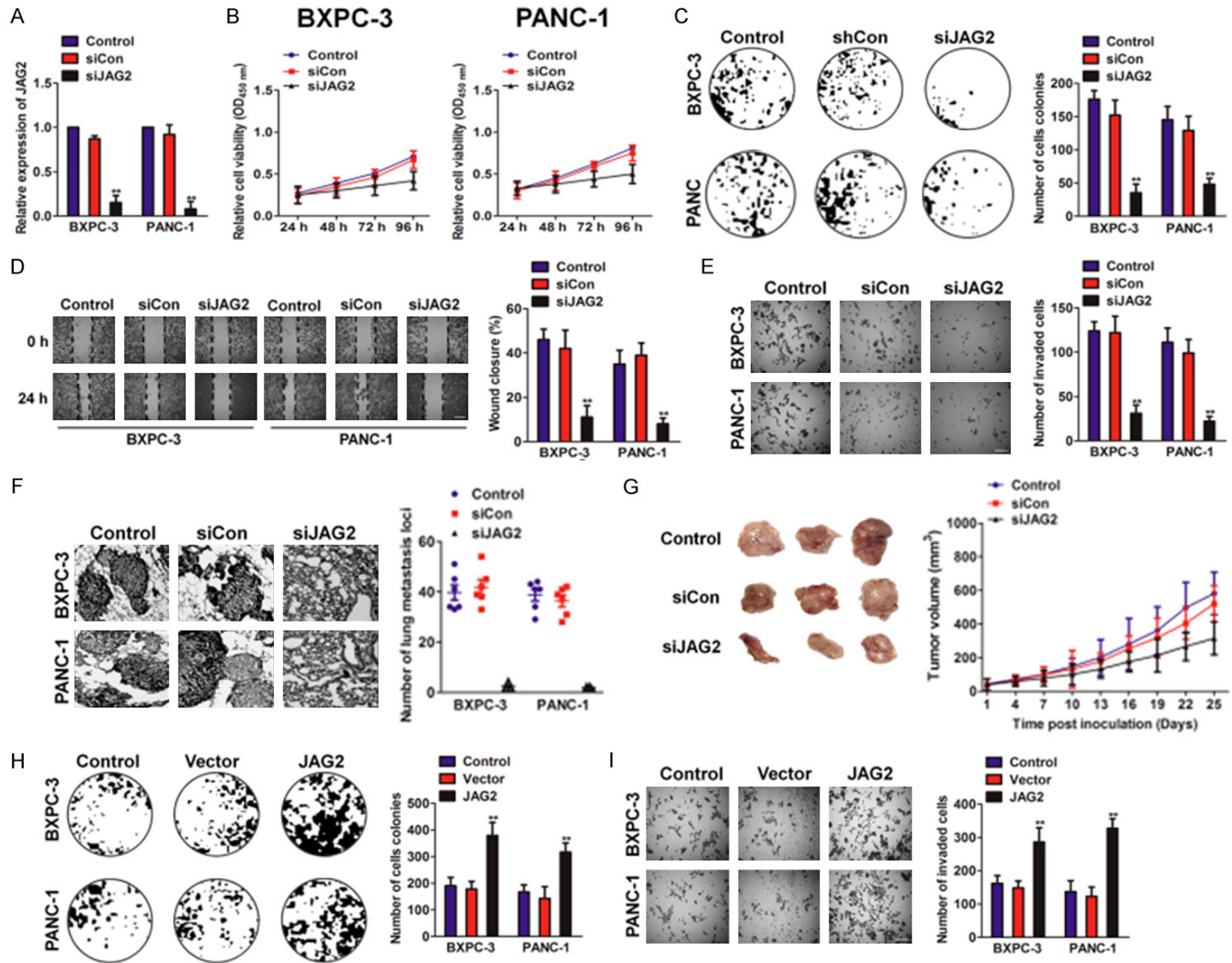


Figure 3. Loss of expression of JAG2 inhibits pancreatic cancer cells growth and metastasis. A. BXPC-3 and PANC-1 cells were transfected with either the negative control siRNA (siCon) or siJAG2. The expression levels of JAG2 were detected by qRT-PCR assay. B. After transfected with siCon or siJAG2, the cell proliferation rates were determined by the MTT assay. C. Colony formation assays of BXPC-3 and PANC-1 cells. Representative images for each treatment were shown. D. BXPC-3 and PANC-1 cells were transfected with siJAG2 and the ability of migration was determined by wound scratch assay. Scale bar: 200 μ m. E. Pancreatic cancer cells with silent expression of JAG2 exhibit less invasive abilities in Transwell invasion assay. The invaded cells were stained with crystal violet and counted. Scale bar: 200 μ m. F. siJAG2 cells or control cells were injected into nude mice via lateral vein. Representative pictures of lungs from mice were taken after four weeks. Numbers of lung metastasis were quantified. G. Knocked-down of JAG2 inhibited the growth of pancreatic cancer cells-engrafted tumors. Representative tumors were photographed at 25 days after mice inoculation with siJAG2 or control cells. H. BXPC-3 and PANC-1 cells were transfected with either the control vector or JAG2. Colony formation assays of BXPC-3 and PANC-1 cells. Representative images for each treatment were shown. I. BXPC-3 and PANC-1 cells were transfected with either the control vector or JAG2. The invasion of pancreatic cancer cells was determined by Transwell invasion assay. Scale bar: 200 μ m. ** $P < 0.01$ as compared to control cells.

JAG2-knockdown in BXPC-3 and PANC-1 cells inhibited cell growth and colony formation in vitro (**Figure 3B, 3C**). Consistently, mobility and invasion were also significantly suppressed by siJAG2 (**Figure 3D, 3E**). To investigate the role of JAG2 in pancreatic cancer cell metastasis, the experimental metastasis assay was conducted. JAG2-knockdown or control cells were injected into nude mice via the lateral tail vein. Four weeks post inoculation, injection of parental cells resulted in the formation of numerous metastatic loci, whereas silencing of JAG2 markedly inhibited pulmonary metastasis (**Figure 3F**). We also evaluated the function of JAG2 in the growth of human pancreatic cancer cell xenografts in nude mice. Parental or JAG2-knockdown PANC-1 cells were injected subcutaneously into nude mice. The tumor sizes and weights were obviously suppressed in the JAG2-downregulated group when compared to the control (**Figure 3G**). To further confirm the potential role of JAG2 in cell growth and mobility, both BXPC-3 and PANC-1 cells were transfected either with a control vector or JAG2 (in order to overexpress the level of JAG2). As expected, overexpression of JAG2 remarkably accelerated the growth and invasion of BXPC-3 and PANC-1 cells as determined by the MTT assay (**Figure 3H**) and Transwell invasion analysis (**Figure 3I**). These results implied that JAG2 silencing perturbed the growth and metastasis of pancreatic cancer cells, which was a similar effect exhibited by overexpressed miR-876-3p.

JAG2 overexpression rescues the effects of miR-876-3p in pancreatic cancer cells

To investigate the functional relevance of JAG2 targeting by miR-876-3p, we assessed if JAG2 overexpression could rescue the inhibitory effects of miR-876-3p on BXPC-3 and PANC-

1 cell proliferation, apoptosis, migration, and invasion. BXPC-3 and PANC-1 cells were co-transfected with miR-876-3p mimics and JAG2 overexpression plasmids. qRT-PCR analysis was used to validate the JAG2 mRNA in the rescue experiment (**Figure 4A**). MTT analysis suggested that the exogenous expression of JAG2 rescued the inhibitory effect of miR-876-3p on cell proliferation in vitro (**Figure 4B**). To elucidate the functions of miR-876-3p/JAG2, we conducted a colony formation assay. As shown in **Figure 4C**, miR-876-3p significantly inhibited colony formation in BXPC-3 and PANC-1 cells with the miR-876-3p mimic, whereas JAG2 rescued colony formation in pancreatic cancer. Consistently, apoptosis in miR-876-3p-transfected BXPC-3 and PANC-1 cells was significantly lowered by JAG2 (**Figure 4D**). After co-transfection with the miR-876-3p mimic and JAG2 overexpression plasmid, both BXPC-3 and PANC-1 cells were subjected to the wound healing and Transwell invasion assay. As shown in **Figure 4E, 4F**, the mobility and invasive capacity inhibited by miR-876-3p was remarkably rescued by the overexpression of JAG2.

Knockdown of JAG2 reverses the effects of miR-876-3p inhibition in pancreatic cancer cells

Next, we explored if JAG2 knockdown could reverse the effects of miR-876-3p loss on BXPC-3 and PANC-1 cell proliferation, migration, and invasion. BXPC-3 and PANC-1 cells were co-transfected with anti-miR-876-3p and/or JAG2 siRNA (siRNA). The levels of JAG2 in both cell lines were verified at the mRNA level (**Figure 5A**). MTT and colony formation assays were also conducted to determine if siJAG2 reversed the inhibitory effects of miR-876-3p loss on BXPC-3 and PANC-1 cell growth in vivo.

miR-876-3p inhibits pancreatic adenocarcinoma progression

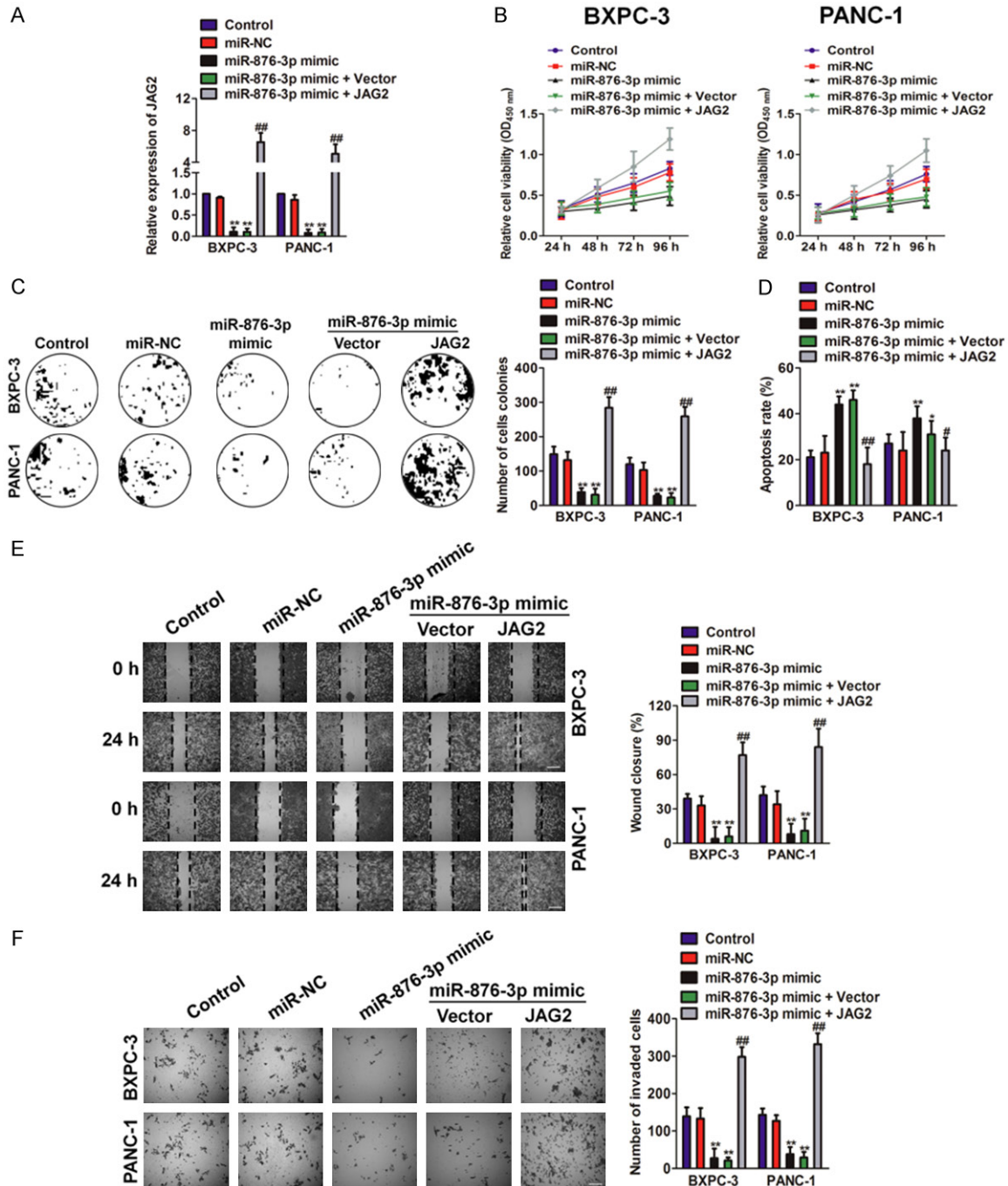


Figure 4. Up-regulation of JAG2 rescues the effects of miR-876-3p. A. PANC-1 and BXPC-3 cells were transfected with miR-876-3p mimic, or co-transfected with JAG2 over-expression plasmid and miR-876-3p mimic. JAG2 expression on mRNA levels by qRT-PCR assay. B. Cells were transfected with miR-876-3p mimic alone, or co-transfected with JAG2 and miR-876-3p mimic, and then were seeded into 96 well plates. After 24 h, 48 h, 72 h and 96 h, the MTT assay was performed to analysis cell proliferation. C. Colony formation assays of BXPC-3 and PANC-1 cells. Representative images for each treatment were shown. D. The apoptosis rate was analyzed by flow cytometry following co-transfection with JAG2 and miR-876-3p into cells. E. BXPC-3 and PANC-1 cells co-transfected with JAG2 over-expression plasmid and miR-876-3p were subjected to wound healing assay and images were taken at 0 and 24 h (left panel). The percentage of wound closure was quantified (right panel). F. Transwell invasion assay was performed after transfection of BXPC-3 and PANC-1 cells with JAG2 plasmid and miR-876-3p mimic. The invaded cells were stained with crystal violet and counted. * $P < 0.05$, ** $P < 0.01$ as compared to control, # $P < 0.05$, ## $P < 0.01$ as compared to miR-876-3p mimic.

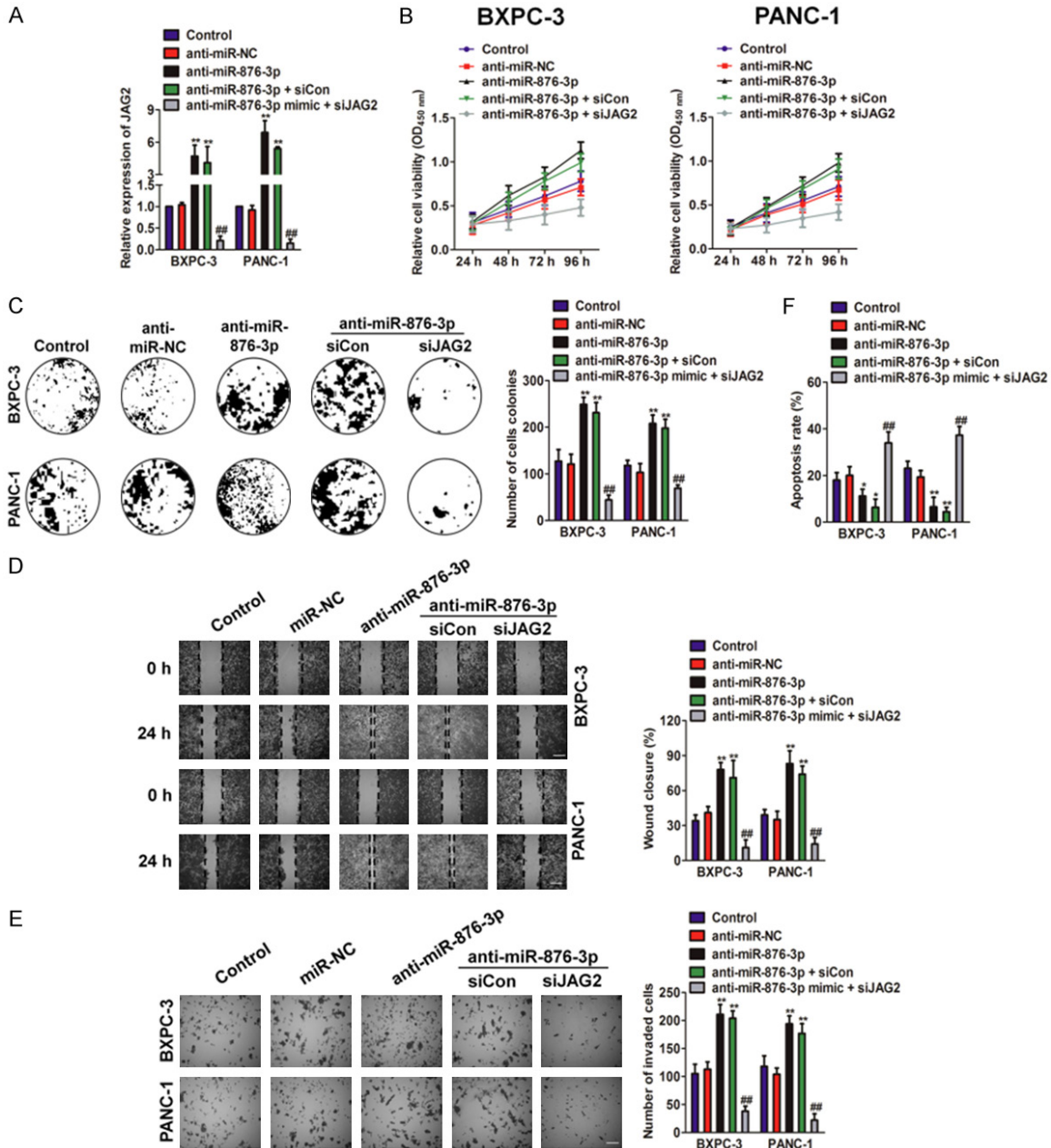


Figure 5. JAG2 knock-down reversed the effects of miR-876-3p inhibition in pancreatic cancer. **A.** PANC-1 and BXPC-3 cells were transfected with anti-miR-876-3p, co-transfected with siJAG2 and anti-miR-876-3p. The expression of JAG2 was determined by qRT-PCR analysis. **B.** Both BXPC-3 and PANC-1 cells were transfected with anti-miR-876-3p, or co-transfected with siJAG2 and anti-miR-876-3p, and then were seeded into 96 well plates. After 24 h, 48 h, 72 h and 96 h, the MTT assay was performed to analysis cell proliferation. **C.** Colony formation assays of BXPC-3 and PANC-1 cells. Representative images for each treatment were shown. **D.** BXPC-3 and PANC-1 cells co-transfected with siJAG2 and anti-miR-876-3p were subjected to wound closure assay. The percentage of wound closure was quantified (right panel). Scale bar: 200 μ m. **E.** Transwell invasion assay was performed after transfection of BXPC-3 and PANC-1 cells with siJAG2 and anti-miR-876-3p. The invaded cells were stained with crystal violet and counted. Scale bar: 200 μ m. **F.** The rate of apoptosis was analyzed by flow cytometry following co-transfection with siJAG2 and anti-miR-876-3p in BXPC-3 and PANC-1 cells. * $P < 0.01$, ** $P < 0.01$ as compared to control and ## $P < 0.01$ as compared to anti-miR-876-3p.

As shown in **Figure 5B** and **5C**, JAG2 knock-down reversed all the effects of miR-876-3p

loss with respect to cell proliferation and colony formation. Consistently, cells transfected with

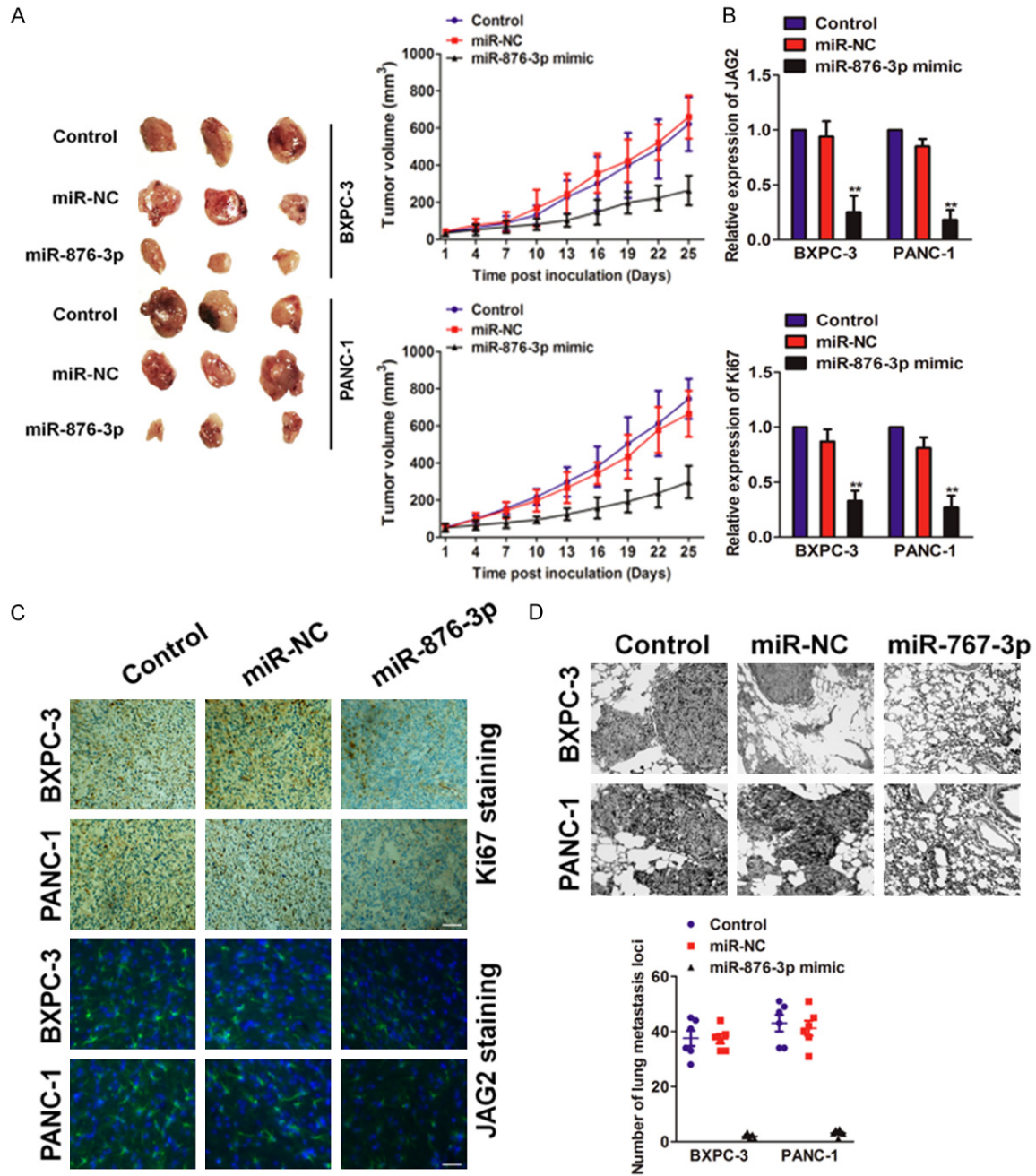


Figure 6. Up-regulation of miR-876-3p inhibits pancreatic cancer cells growth and metastasis in vivo. **A.** miR-876-3p stably over-expressing or parental pancreatic cancer cells were injected into nude mice by subcutaneous. Tumor volumes were measured and growth curves were generated. **B.** The expression of miR-876-3p and JAG2 was determined by qRT-PCR assay in the tumor tissues formed by miR-876-3p over-expression cells and parental cells. **C.** The expression of Ki67 and JAG2 in tumor mass was detected by immunohistochemistry and immunofluorescence assay, respectively. **D.** The numbers of lung metastatic nodes of lungs from mice induced by miR-876-3p stably over-expressing or parental pancreatic cancer cells were displayed. Histopathology of metastasis was determined with H&E staining. ** $P < 0.01$ compared to control group.

siJAG2 had their mobility and invasive capacities restored in the presence of anti-miR-876-3p (Figure 5D, 5E). Furthermore, the apoptosis levels increased in cells co-transfected with

siJAG2 and anti-miR-876-3p (Figure 5F). These results suggested that miR-876-3p influenced the growth and aggressiveness of BXPC-3 and PANC-1 cells by targeting JAG2.

miR-876-3p inhibits pancreatic adenocarcinoma progression

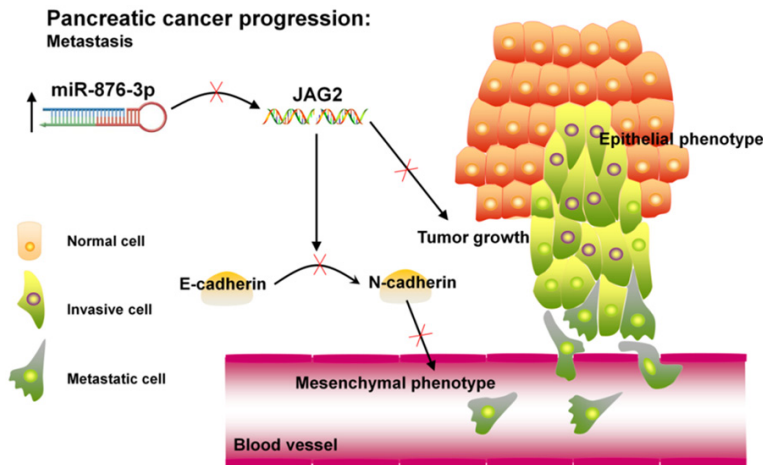


Figure 7. Proposed model by which miR-876-3p inhibits the progression of pancreatic adenocarcinoma by targeting JAG2.

MiR-876-3p suppresses tumor growth and metastasis in pancreatic cancer xenograft models

To examine the precise role of miR-876-3p *in vivo*, nude mice were subcutaneously inoculated with miR-876-3p-overexpressing pancreatic cancer cells or control cells. The miR-876-3p-overexpressing xenograft group exhibited significant tumor growth inhibition when compared to the control group (**Figure 6A**). Moreover, a marked up-regulation of miR-876-3p and a remarkable down-regulation of JAG2 were found in the tumor masses of the mice inoculated with miR-876-3p-overexpressing pancreatic cancer cells when compared to the control group (**Figure 6B**). Subsequently, we measured the levels of Ki67 and JAG2 in the tumor masses using immunohistochemistry and immunofluorescence assays, respectively. As shown in **Figure 6C**, tumor tissues from stable miR-876-3p-overexpressing cells exhibited a significant down-regulation of Ki67 and JAG2. These results suggested that miR-876-3p inhibited tumor growth *in vivo*, which was consistent with the functional results *in vitro*. To ascertain if miR-876-3p affected tumor metastasis *in vivo*, miR-876-3p-overexpressing pancreatic cancer cells or parental cells were injected into nude mice via the tail vein. Four weeks after tail vein injection, a marked effect was discovered on the number of metastatic nodes formed in the lung tissues (**Figure 6D**).

Discussion

Accumulating evidence shows that miRNAs are involved in tumorigenesis and metastasis of

various cancers, including pancreatic cancer [18]. miRNAs have also been implicated to function as both tumorigenic and tumor-suppressing genes. Metastasis is characteristic of pancreatic cancer and a crucial step in pancreatic cancer progression. A substantial amount of evidence indicates that miRNAs contribute to tumor evolution; however, the capacity in which specific miRNAs function in pancreatic cancer metastasis still remains undefined [19]. Here, we identified a panel of abnormally expressed miRNAs in pancreatic carcinoma, such as miR-

146a, miR-501-3p, and miR-199a [20-22]. These miRNAs regulate the malignant progression of pancreatic cancer by targeting specific genes (EGFR, E-cadherin, and mTOR). Our study identified that miR-876-3p acted as an overexpressed suppressor gene in pancreatic carcinoma, and was involved in the growth and metastasis of pancreatic cancer cells. It is the first study to reveal that the JAG2 gene is negatively regulated by miR-876-3p via a specific target site within the 3'-UTR region of the JAG2 gene (**Figure 7**).

In the present study, we verified that miR-876-3p was remarkably down-regulated in pancreatic cancer tissues and cell lines when compared to normal controls. Furthermore, we demonstrated that the induced expression of miR-876-3p in pancreatic carcinoma markedly inhibited the cell growth and metastatic phenotype. Moreover, the external down-regulation of miR-876-3p significantly hindered pancreatic cancer cell proliferation and mobility *in vitro*. Stable depletion of miR-876-3p suppressed the tumorigenicity of pancreatic cancer cells in nude mice. Additionally, metastatic nodules in the lung, derived from the miR-876-3p-transfected cells, were markedly fewer than that in controls. Mechanistically, we determined JAG2 to be a direct target of miR-876-3p, and its expression was inversely correlated with the level of miR-876-3p in pancreatic cancer.

As noncoding RNAs, miRNAs execute their functions by targeting protein-coding genes. JAG2 is reported to be most commonly altered in solid tumors. It is significantly up-regulated in

colorectal cancer when compared to normal tissues, and JAG2 downregulation inhibits the invasiveness of colorectal cancer cell lines without significantly affecting cell growth [11]. These findings implicate JAG2 in promoting the aggressiveness of colorectal cancers, and lay the foundation for its future development as a therapeutic target in colorectal cancer treatment. JAG2 has also been linked to the metastasis of epithelium-derived tumors such as lung cancer, breast cancer, colon cancer, and urothelial carcinoma of the bladder [23]. Although human JAG1 mRNA has been shown to be expressed in embryonic stem cells, neural tissues, lung carcinoids, gastric cancers, pancreatic cancers, colon cancers, and squamous cell carcinomas of the skin, oral cavity, esophagus, head, and neck [24], very little research highlights the potential role of JAG2 in pancreatic cancer metastasis. We studied the function of JAG2 in pancreatic cancer and proved that its knockdown significantly repressed pancreatic cancer cell growth, migration, and invasion. Cumulatively, we reveal an important miRNA-involved pathway that regulates tumor cell growth, apoptosis, and metastasis in pancreatic cancer. Therefore, it would be beneficial to involve miR-876-3p in clinical research so as to determine its therapeutic applications in pancreatic and other cancers.

Disclosure of conflict of interest

None.

Address correspondence to: De Quan Jiang, The Second Department of General Surgery of Jiangjin Center Hospital, Chongqing, China. E-mail: jiangdequanjdq@hotmail.com

References

[1] Fiorino S, Bacchi-Reggiani ML, Birtolo C, Acquaviva G, Visani M, Fornelli A, Masetti M, Tura A, Sbrignadello S, Grizzi F, Patrinoicola F, Zanello M, Mastrangelo L, Lombardi R, Benini C, Di Tommaso L, Bondi A, Monetti F, Siopis E, Orlandi PE, Imbriani M, Fabbri C, Giovanelli S, Domanico A, Accogli E, Di Saverio S, Grifoni D, Cennamo V, Leandri P, Jovine E and de Biase D. Matricellular proteins and survival in patients with pancreatic cancer: a systematic review. *Pancreatology* 2018; 18: 122-132.

[2] Omura N and Goggins M. Epigenetics and epigenetic alterations in pancreatic cancer. *Int J Clin Exp Pathol* 2009; 2: 310-326.

[3] Okui M, Yamamichi T, Asakawa A, Harada M and Horio H. Resection for pancreatic cancer lung metastases. *Korean J Thorac Cardiovasc Surg* 2017; 50: 326-328.

[4] Walling A and Freelove R. Pancreatitis and pancreatic cancer. *Prim Care* 2017; 44: 609-620.

[5] Liu L, Yao D, Zhang P, Ding W, Zhang X, Zhang C, Gong S, Zhang Y, Wang J, Sun T and Ren Z. Deubiquitinase USP9X promotes cell migration, invasion and inhibits apoptosis of human pancreatic cancer. *Oncol Rep* 2017; 38: 3531-3537.

[6] Kim YJ, Jeong SH, Kim EK, Kim EJ and Cho JH. Ursodeoxycholic acid suppresses epithelial-mesenchymal transition and cancer stem cell formation by reducing the levels of peroxiredoxin II and reactive oxygen species in pancreatic cancer cells. *Oncol Rep* 2017; 38: 3632-3638.

[7] Yin S, Bleul T, Zhu Y, Isayev O, Werner J and Bazhin AV. MiRNAs are unlikely to be involved in retinoid receptor gene regulation in pancreatic cancer cells. *Cell Physiol Biochem* 2017; 44: 644-656.

[8] Liu R, Zhang H, Wang X, Zhou L, Li H, Deng T, Qu Y, Duan J, Bai M, Ge S, Ning T, Zhang L, Huang D and Ba Y. The miR-24-Bim pathway promotes tumor growth and angiogenesis in pancreatic carcinoma. *Oncotarget* 2015; 6: 43831-43842.

[9] Asnaghi L, Handa JT, Merbs SL, Harbour JW and Eberhart CG. A role for Jag2 in promoting uveal melanoma dissemination and growth. *Invest Ophthalmol Vis Sci* 2013; 54: 295-306.

[10] Wang F, Remke M, Bhat K, Wong ET, Zhou S, Ramaswamy V, Dubuc A, Fonkem E, Salem S, Zhang H, Hsieh TC, O'Rourke ST, Wu L, Li DW, Hawkins C, Kohane IS, Wu JM, Wu M, Taylor MD and Wu E. A microRNA-1280/JAG2 network comprises a novel biological target in high-risk medulloblastoma. *Oncotarget* 2015; 6: 2709-2724.

[11] Vaish V, Kim J and Shim M. Jagged-2 (JAG2) enhances tumorigenicity and chemoresistance of colorectal cancer cells. *Oncotarget* 2017; 8: 53262-53275.

[12] Xishan Z, Bin Z, Haiyue Z, Xiaowei D, Jingwen B and Guojun Z. Jagged-2 enhances immunomodulatory activity in adipose derived mesenchymal stem cells. *Sci Rep* 2015; 5: 14284.

[13] Hsu YL, Wu CY, Hung JY, Lin YS, Huang MS and Kuo PL. Galectin-1 promotes lung cancer tumor metastasis by potentiating integrin alpha6beta4 and Notch1/Jagged2 signaling pathway. *Carcinogenesis* 2013; 34: 1370-1381.

[14] Zheng SY, Li Y, Jiang D, Zhao J and Ge JF. Anti-cancer effect and apoptosis induction by quer-

miR-876-3p inhibits pancreatic adenocarcinoma progression

- cetin in the human lung cancer cell line A-549. *Mol Med Rep* 2012; 5: 822-826.
- [15] Lv G, Tan Y, Lv H, Fang T, Wang C, Li T, Yu Y, Hu C, Wen W, Wang H and Yang W. MXR7 facilitates liver cancer metastasis via epithelial-mesenchymal transition. *Sci China Life Sci* 2017; 60: 1203-1213.
- [16] Li Q, Yao L, Wei Y, Geng S, He C and Jiang H. Role of RHOT1 on migration and proliferation of pancreatic cancer. *Am J Cancer Res* 2015; 5: 1460-1470.
- [17] Fan Y, Yin S, Hao Y, Yang J, Zhang H, Sun C, Ma M, Chang Q and Xi JJ. miR-19b promotes tumor growth and metastasis via targeting TP53. *RNA* 2014; 20: 765-772.
- [18] Wang Z, Liu Z, Fang X and Yang H. MiR-142-5p suppresses tumorigenesis by targeting PIK3CA in non-small cell lung cancer. *Cell Physiol Biochem* 2017; 43: 2505-2515.
- [19] Liu D, Zhang J, Wu Y, Shi G, Yuan H, Lu Z, Zhu Q, Wu P, Lu C, Guo F, Chen J, Jiang K and Miao Y. YY1 suppresses proliferation and migration of pancreatic ductal adenocarcinoma by regulating the CDKN3/Mdm2/P53/P21 signaling pathway. *Int J Cancer* 2018; 142: 1392-1404.
- [20] Ali S, Ahmad A, Aboukameel A, Ahmed A, Bao B, Banerjee S, Philip PA and Sarkar FH. Deregulation of miR-146a expression in a mouse model of pancreatic cancer affecting EGFR signaling. *Cancer Lett* 2014; 351: 134-142.
- [21] Ling Q, Xu X, Ye P, Xie H, Gao F, Hu Q, Liu Z, Wei X, Roder C, Trauzold A, Kalthoff H and Zheng S. The prognostic relevance of primary tumor location in patients undergoing resection for pancreatic ductal adenocarcinoma. *Oncotarget* 2017; 8: 15159-15167.
- [22] Kuninty PR, Bojmar L, Tjomsland V, Larsson M, Storm G, Ostman A, Sandstrom P and Prakash J. MicroRNA-199a and -214 as potential therapeutic targets in pancreatic stellate cells in pancreatic tumor. *Oncotarget* 2016; 7: 16396-16408.
- [23] Choi K, Ahn YH, Gibbons DL, Tran HT, Creighton CJ, Girard L, Minna JD, Qin FX and Kurie JM. Distinct biological roles for the notch ligands Jagged-1 and Jagged-2. *J Biol Chem* 2009; 284: 17766-17774.
- [24] Sugiyama M, Oki E, Nakaji Y, Tsutsumi S, Ono N, Nakanishi R, Sugiyama M, Nakashima Y, Sonoda H, Ohgaki K, Yamashita N, Saeki H, Okano S, Kitao H, Morita M, Oda Y and Maebara Y. High expression of the Notch ligand Jagged-1 is associated with poor prognosis after surgery for colorectal cancer. *Cancer Sci* 2016; 107: 1705-1716.

miR-876-3p inhibits pancreatic adenocarcinoma progression

Supplementary Table 1. Significant miRNA expression profiles in normal tissues compared to pancreatic adenocarcinoma

Row. Names (tT)	logFC	AveExpr	t	P. Value	adj.P.Val
hsa-miR-130b	3.917266	7.146485	11.03274	5.91E-21	6.26E-19
hsa-miR-148a	4.651428	7.767239	9.989179	2.03E-18	1.84E-16
hsa-miR-217	5.425394	7.068048	10.18674	3.56E-17	2.83E-15
hsa-miR-30c	1.649024	10.05073	8.501457	1.14E-14	7.28E-13
hsa-miR-30b	1.671635	9.524101	8.329831	3.17E-14	1.84E-12
hsa-miR-30a	1.577212	10.78951	7.889348	4.19E-13	1.78E-11
hsa-miR-192	3.02832	7.954379	7.396891	1.09E-11	3.85E-10
hsa-miR-216a	4.742841	8.522703	7.558372	2.99E-11	1.00E-09
hsa-miR-216b	4.298115	9.767851	7.340633	1.19E-10	3.80E-09
hsa-miR-215	2.798319	6.622068	6.955732	1.94E-10	5.88E-09
hsa-miR-130a	1.593661	8.434754	6.547287	7.40E-10	1.88E-08
hsa-miR-200c	1.856217	12.51612	6.176459	5.16E-09	1.03E-07
hsa-miR-29c	1.8219	8.158036	6.124632	7.03E-09	1.36E-07
hsa-miR-30e	1.686805	8.107792	6.031927	1.08E-08	2.01E-07
hsa-miR-200b	1.397991	11.05577	5.240878	4.99E-07	8.14E-06
hsa-miR-182	2.684717	6.07872	5.283826	5.95E-07	9.28E-06
hsa-miR-365	1.70541	5.945926	5.222554	5.98E-07	9.28E-06
hsa-miR-141	2.358239	5.19218	4.311953	4.81E-05	0.000557
hsa-miR-200a	1.881522	7.622773	4.171723	5.26E-05	0.000598
hsa-miR-375	2.112092	11.32874	4.126916	6.12E-05	0.000683
hsa-miR-195	1.079182	8.663077	4.043716	8.19E-05	0.000882
hsa-miR-376c	2.631982	4.632892	3.931133	0.000211	0.002063
hsa-miR-194	1.642947	8.64004	3.844186	0.000178	0.001796
hsa-miR-126	1.086069	9.59825	3.802932	0.000202	0.002006
hsa-miR-29b	1.762353	5.493678	3.619745	0.000465	0.004054
hsa-miR-381	3.225684	4.766494	3.857911	0.001425	0.010922
hsa-miR-425*	1.053873	6.61702	3.264834	0.001348	0.010458
hsa-miR-30a*	1.329956	5.570819	3.257648	0.001598	0.01182
hsa-miR-376a	1.243557	5.762811	3.24606	0.001458	0.01104
hsa-miR-379	1.074936	5.469563	3.060724	0.002755	0.018251
hsa-miR-921	1.910478	4.029455	2.92405	0.004756	0.029657
hsa-miR-1181	1.350198	4.825974	2.971022	0.003616	0.02277
hsa-miR-191*	1.185364	7.351562	2.997111	0.003212	0.020682
hsa-miR-604	1.247448	6.303192	2.989403	0.003272	0.020808
hsa-miR-148a*	1.462124	3.964764	2.893233	0.005773	0.035647
hsa-miR-634	1.160289	8.045452	2.751789	0.006675	0.039674
hsa-miR-513b	1.590336	5.593478	2.732149	0.007467	0.043572
hsa-miR-181a	-3.30759	10.74993	-12.441	2.13E-25	1.35E-22
hsa-miR-181b	-2.57839	9.018058	-11.5277	8.62E-23	2.74E-20
hsa-miR-214	-3.26483	10.29873	-11.4049	1.75E-22	3.70E-20
hsa-miR-222	-2.3965	10.21791	-10.8971	4.12E-21	6.26E-19
hsa-miR-181c	-3.3055	9.105183	-10.9087	5.70E-21	6.26E-19
hsa-miR-150	-3.32835	9.219503	-8.54803	8.67E-15	6.13E-13
hsa-miR-155	-3.57978	9.33456	-8.35824	3.77E-14	2.00E-12
hsa-miR-221	-1.80344	10.50387	-8.15909	8.69E-14	4.25E-12
hsa-miR-125b	-1.32523	13.43076	-8.04587	1.69E-13	7.66E-12
hsa-let-7i	-1.30842	11.85257	-7.63137	1.85E-12	7.36E-11

miR-876-3p inhibits pancreatic adenocarcinoma progression

hsa-miR-145	-1.74888	11.43106	-7.40159	6.82E-12	2.55E-10
hsa-miR-324-5p	-1.94738	6.451429	-6.8051	2.23E-10	6.45E-09
hsa-miR-23a	-1.01567	12.96179	-6.73031	2.75E-10	7.29E-09
hsa-miR-181d	-2.60422	7.272766	-6.48941	1.28E-09	3.14E-08
hsa-miR-15b	-1.44279	10.5312	-6.4194	1.47E-09	3.46E-08
hsa-miR-93	-1.14862	9.920712	-6.37706	1.79E-09	4.06E-08
hsa-miR-92a	-1.7312	9.493539	-6.30408	2.65E-09	5.80E-08
hsa-miR-199a-5p	-1.68894	8.629875	-6.24877	3.48E-09	7.38E-08
hsa-miR-199b-3p	-1.2218	11.66628	-6.20677	4.32E-09	8.87E-08
hsa-miR-199a-3p	-1.2261	11.27671	-5.72	4.98E-08	8.80E-07
hsa-miR-1246	-1.97009	7.48921	-5.29905	4.15E-07	6.95E-06
hsa-miR-210	-3.57998	6.966041	-5.19735	8.60E-07	1.30E-05
hsa-miR-324-3p	-2.97984	5.287184	-5.18364	9.04E-07	1.34E-05
hsa-miR-532-3p	-1.62115	6.052223	-5.03785	1.35E-06	1.96E-05
hsa-miR-409-3p	-2.18896	6.077698	-5.02788	1.46E-06	2.05E-05
hsa-miR-132	-1.80545	7.983975	-4.90178	2.36E-06	3.20E-05
hsa-miR-146a	-1.82301	8.239321	-4.67538	6.37E-06	8.27E-05
hsa-miR-423-3p	-1.04198	8.711237	-4.68729	5.84E-06	7.74E-05
hsa-miR-652	-1.40013	6.678759	-4.67185	6.56E-06	8.35E-05
hsa-miR-874	-2.38567	5.29416	-4.56152	1.21E-05	0.000148
hsa-miR-345	-7.94748	3.235472	-4.54176	3.67E-05	0.000441
hsa-miR-31	-3.44388	8.803117	-4.006	0.000109	0.001137
hsa-miR-518b	-8.00298	2.971412	-4.89411	7.93E-05	0.000869
hsa-miR-125a-5p	-1.16489	10.60987	-3.99028	9.96E-05	0.001056
hsa-miR-1279	-8.81454	3.548614	-4.88643	0.000144	0.001482
hsa-miR-155*	-8.02764	2.878748	-4.58067	0.000239	0.002236
hsa-miR-523	-8.47359	3.094854	-4.84673	0.000223	0.002147
hsa-miR-10a	-1.03615	8.516233	-3.76794	0.000231	0.002194
hsa-miR-101*	-5.44492	3.907203	-3.89011	0.000544	0.004678
hsa-miR-30d*	-8.31915	3.193545	-4.2466	0.000447	0.003948
hsa-miR-331-3p	-1.06019	7.794788	-3.62336	0.000389	0.003585
hsa-miR-876-3p	-9.97301	2.948378	-5.45406	0.000442	0.003948
hsa-miR-26a-2*	-8.46606	3.165034	-4.04357	0.000967	0.007886
hsa-miR-501-3p	-2.1044	4.564446	-3.4326	0.000832	0.006964
hsa-miR-744	-1.43407	5.671904	-3.39409	0.000906	0.007487
hsa-miR-632	-8.72398	3.521523	-3.65546	0.001842	0.013161
hsa-miR-484	-1.13572	6.570759	-3.34323	0.001037	0.00835
hsa-miR-92b	-1.30958	6.265604	-3.28586	0.001285	0.010094
hsa-miR-571	-8.01898	1.482855	-4.34762	0.001974	0.013796
hsa-miR-432	-2.13644	5.010935	-3.16357	0.002206	0.015248
hsa-miR-502-3p	-1.25662	5.802865	-3.21188	0.00166	0.012136
hsa-miR-886-5p	-2.25438	5.926714	-3.00817	0.00318	0.020682
hsa-miR-26a-1*	-4.21596	3.285377	-2.92571	0.006297	0.038508
hsa-miR-127-3p	-1.16364	7.824259	-2.9924	0.003219	0.020682